

FREQUENCY DOMAIN MODELLING AND IDENTIFICATION OF 2D DIGITAL SERVO VALVE

Jian Ruan¹, Paul R. Ukrainetz² and Richard Burton²

¹ Department of Mechanical Engineering, Zhejiang University of Technology, Hangzhou 310014, P.R. China

² Department of Mechanical Engineering, University of Saskatchewan, 57 Campus Drive, Saskatoon, Saskatchewan, Canada, S7N 5A9
wxmin@public.hz.zj.cn, burton@enr.usask.ca

Abstract

The 2D digital servo valve studied here is a two-stage valve designed by using both rotary (angular) and linear motions of a spool. The rotary motion is driven by a stepper motor operating under continual angular displacement control, while the linear motion of the spool is actuated by hydraulic servo control with feedback of the spool's displacement, which is achieved by a unique "servo screw".

The modelling of the 2D valve is based on linear theory and is further verified by the special experiments. Because of the extremely large hydraulic natural frequency, the control of the 2D valve is identified as being that of a first-order-system. The relation between the time constant and the structural parameters is established, accounting for the non-linearity of the pilot hydraulic bridge. For the continual control of the stepper motor, a mathematical model considering the rotary motion, the rotating magnetic field and the angular control signal is established. In order to prevent the stepper motor from losing steps, the rate of the control signal is limited to a certain range. As a result, this may cause a non-linearity and, consequently, the deformation of the waveform when the input sinusoid wave is of large amplitude and high frequency. By utilizing the method of the description function, the effect of limiting the rate of the control signal is approximated as a first-order-system and the relation between the time constant and the amplitude and frequency is presented. The dynamic characteristics of the stepper motor are to a large extent dependent upon the way the power is supplied. For a constant current supply, the stepper motor can be classified as a second-order-system. The factors affecting the natural frequency and damping ratio are clarified. Finally, the frequency response of the 2D digital valve is experimentally measured and compared with theoretical results. Both theoretical and experimental results show that the 2D digital valve has a fairly high frequency response, especially when the valve operates near the central position. For a 25% full scale input signal, the 2D digital servo valve has at least 300 Hz under the gain of -3 dB.

Keywords: servo valve, digital control, dynamic modelling, frequency response

1 Introduction

The performance of an electrohydraulic servo system is to a large extent dominated by the dynamic response of the servo valve. The conventional nozzle-flapper servo valve demonstrates fairly high frequency response capability due to the small inertia of the armature-flapper assembly (Merritt, 1967), but is sensitive to oil contamination. The proportional valve takes the advantage of dirt-insensitivity over the nozzle-flapper servo valve. But the large armature mass of the electrical magnet limits the frequency response to a comparatively small range. Therefore, it is important to develop new types of servo control components with both high frequency response capability and dirt

tolerance if hydraulic servo control is to remain competitive with other types of servo controls. Actually, a considerable amount of research has been focused on the development of servo control components or control methods that aim to improve both the dynamic characteristics and dirt tolerance. Two direct digital approaches are particularly interesting and seem to be promising.

One approach is the introduction of PWM (Pulse Width Modulation) to an on-off valve. This method takes the advantage of simple construction and provides dirt tolerance. However, the mechanical "on-off" states of the valve will result in pressure pulsation accompanied by loud noise and vibration of the pipelines. Investigations of both the PWM valve (Hesse and Moller, 1972) and the system (Lai et al, 1989; Palanisamy et al, 1981; Tsai and Ukrainetz, 1970) showed

This manuscript was received on 25 May 2000 and was accepted after revision for publication on 3 August 2000

that the dynamic response with PWM control is highly dependent on the modulating frequency, and the system stability is related to the on-off speed of the solenoid valve (Sawamura and Anafusa, 1962). Thus, the regulation of the switching speed of the on-off mechanism is crucial to the successful application of hydraulic PWM control. The introduction of a new electro-mechanical transformer and innovative designs demonstrated a great potential in this respect (Hou et al, 1995).

The second approach is to introduce a stepper motor to actuate the valve or a pilot. Ramachandran et al (1985) developed and evaluated a stepper motor driven two-stage digital valve with mechanical feedback. Yu et al (1997) and Xu and Ruan (1989) have also carried out numerical simulations of such digital valves. This work pointed out that the dynamic response of the digital valves is related to the number of steps of the stepper motor per stroke of the spool. Since these digital valves use stepper motors to translate the input signal into a stepping motion of a spool and the resolution of the valve is decided by the number of steps per stroke, the number of steps corresponding to the full stroke of the spool should be kept large enough to sustain the high resolution of the valve. However, a large number of steps usually result in slow response of the digital valve. Ruan and Burton in 1999 introduced a new method of controlling the stepper motor for the 2D directional valve. The new method aimed at eliminating quantitative error by introducing continual control of the rotating magnetic field, while maintaining the high frequency response of the valve. The nonlinear static and dynamic characteristics of the 2D servo valve were investigated in detail through simulation and special experiments in another paper (Ruan et al, 2000). Several other studies on the digital valves have been completed by the authors and manuscripts based on these works are in the review process for publication. This paper presents the frequency domain modelling and identification of a 2D digital servo valve actuated by a stepper motor under the continual control.

2 The 2D Digital Servo Valve

The 2D digital valve shown in Fig. 1 is composed of a 2D valve and a stepper motor which is connected to the spool through an elastic coupling and actuates the rotary motion of the spool. The elastic coupling has a large twisting stiffness. Thus, for rotary motion the spool and the rotator are considered to be a rigid body. The linear stiffness of the elastic coupling is maintained within an appropriate range to set the spool to the central position when the system loses pressure in an accident (For the normal operation, there is a special initialization program which automatically controls the spool to the central position at the moment the stepper motor is energized). Between the stepper motor and the spool rotary motion is open loop control. In order to maintain both a high resolution and a rapid response of the 2D digital valve, a special control program has been developed for the continual control of stepper motor (Ruan and Burton, 1999).

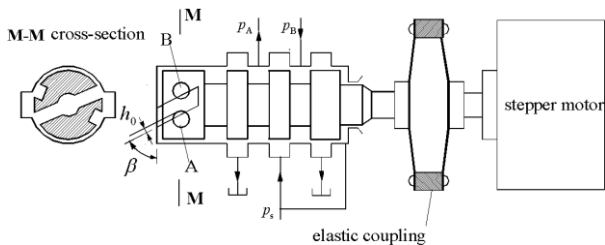


Fig. 1: The 2D digital servo valve

The 2D valve is a two-stage flow rate control valve developed by using both rotary and linear motions of the spool. The right end area of the spool is set to be half of the left one. On the left spool land there are small round holes, labelled A and B, which are connected to the oil supply and the oil tank, respectively. On the left side of the spool cavity there is a spiral groove which is connected to the end of the spool chamber. The holes A and B are located on the two sides of the spiral groove as shown and form two

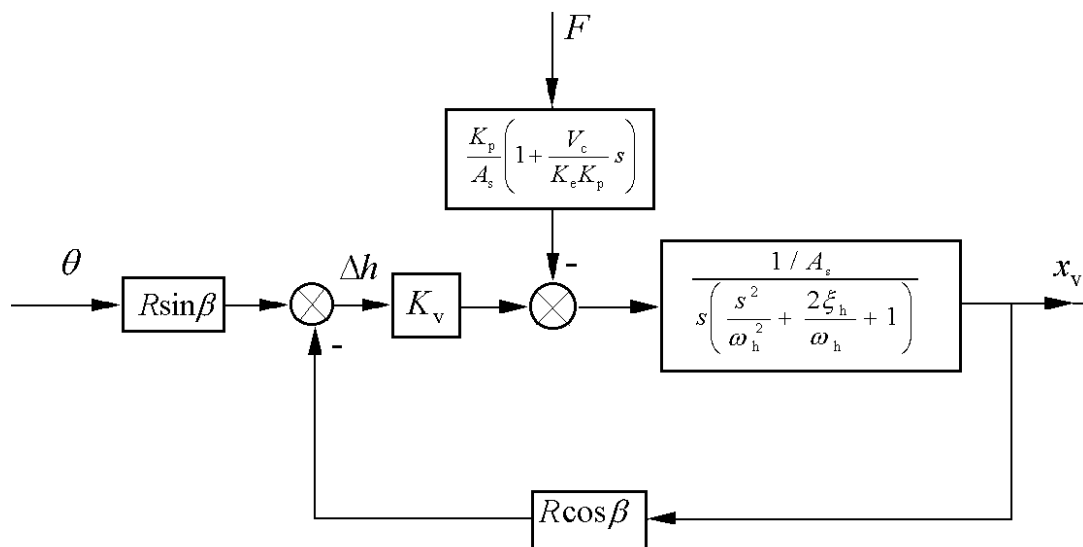


Fig. 2: Signal flow diagram of 2D servo valve

small crescent overlapping openings, which are connected in series to form a hydraulic bridge. The right chamber is connected to the system pressure, while the pressure inside the left chamber is controlled by the hydraulic bridge. Under static conditions, hole A has the same overlap area with respect to the spiral groove as does hole B; the hydraulic bridge gives an output pressure which is equal to the half of system pressure, regardless of Coulomb frictional force and Bernoulli's force. The rotary motion of the spool actuated by the stepper motor will cause the hydraulic bridge, and thus the pressure inside the left chamber, to diverge from the balanced point and consequently result in an imbalance in the hydrostatic force acting across the spool and the consequent linear motion of the spool. The linear motion of the spool will balance the hydraulic bridge and the pressure inside the left chamber will recover to the balanced point.

The 2D valve can be classified as a two-stage flow rate control valve. It is essentially a mechanical hydraulic servo device. The input is the rotary motion of the spool, while the linear is taken as feedback. Thus, the mathematical model of the 2D valve has the same form of a single-action cylinder operated by a three-way-valve (Here, the valve opening is the overlap height of crescent area, Δh). Therefore, the signal flow diagram of the 2D valve in the frequency domain is obtained and shown in Fig. 2 (Merritt, 1967). Based on Fig. 2, the transfer function of the valve can further be simplified. In a practical application, the crescent overlap area is kept very small to reduce the leakage through the hydraulic bridge. The spool has a very large stiffness and the interference of the frictional force F on the linear positioning of the spool is almost negligible (Ruan et al, 2000). Furthermore, the volume of the spool left chamber is designed to be very small and the hydraulic natural frequency, ω_h , is maintained at a very high value (up to $10^4 \sim 10^5$ Hz) and the compressibility of oil becomes negligible. Thus, the second-order-system, as dictated by the spool left chamber and the mass of the spool, has a minor effect on the dynamic characteristics of the valve. In this case, the hydraulic control of the spool is approximated by a

first-order-system as follows:

$$\frac{x_v(s)}{\theta(s)} = \frac{R \tan \beta}{\tau_v s + 1} \quad (1)$$

$$\tau_v = \frac{A_s}{K_q \cos \beta} = \frac{A_s \sqrt{\rho}}{8 K_\lambda C_d \cos \beta \sqrt{p_s (2r_d h_0 - r_d^2 + \delta^2)}} \quad (2)$$

In the expression for the time constant, K_λ is a modifying coefficient that considers the non-linearity of the crescent overlap area. It is obtained by relating the overlap area to the rectangular area, that is:

$$K_\lambda = \frac{\frac{h_0}{r_d} \sqrt{2 \frac{h_0}{r_d} - \left(\frac{h_0}{r_d}\right)^2} + \arcsin \sqrt{2 \frac{h_0}{r_d} - \left(\frac{h_0}{r_d}\right)^2} - \sqrt{2 \frac{h_0}{r_d} - \left(\frac{h_0}{r_d}\right)^2}}{2 \frac{h_0}{r_d} \sqrt{2 \frac{h_0}{r_d} - \left(\frac{h_0}{r_d}\right)^2}} \quad (3)$$

The value of K_λ vs h_0 / r_d is shown in Fig. 3 and is within the range $2/3 \sim \pi/4$ corresponding to the value of h_0 / r_d changing from 0 ~ 1.

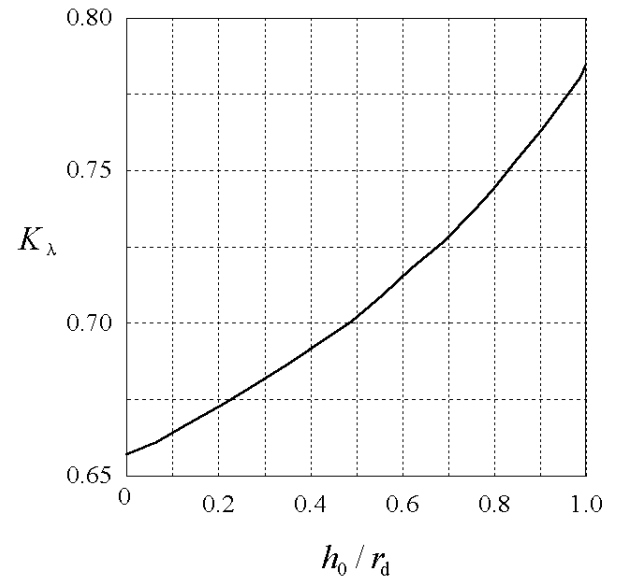


Fig. 3: Curve of K_λ vs h_0 / r_d

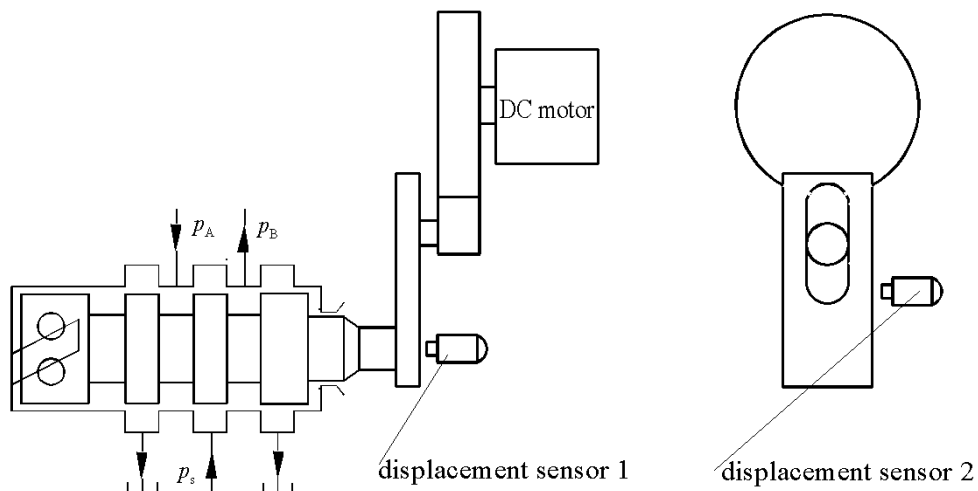


Fig. 4: Experimental arrangement for frequency response of 2D valve

An experiment was designed to obtain the frequency response of the 2D servo valve. The experimental arrangement is illustrated in Fig. 4. An eccentric axis is inserted into the groove on the rod vertically connected to the spool. While the DC motor drives the eccentric axis, the spool will sway to and fro. Because the swaying angular range is small, the rotary motion of the spool approximately takes the form of a sinusoidal wave. The frequency of the sinusoidal wave was adjusted through changing the angular speed of the DC motor. The movements of both rotation and sliding are measured by two eddy-current displacement sensors and recorded on an oscilloscope.

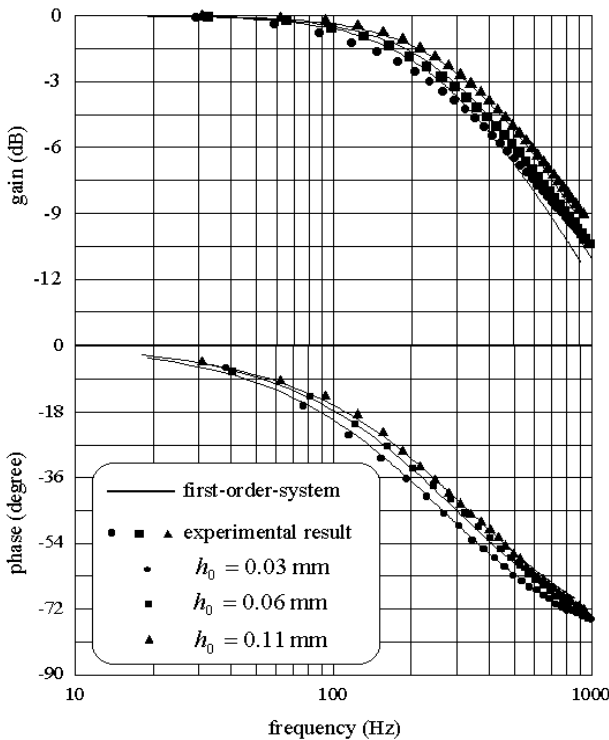


Fig. 5: Frequency response of the 2D servo valve

By obtaining the amplitude variation of the sliding motion and the phase shift between the angular sinusoidal wave and the sliding sinusoidal wave, the frequency response of the 2D servo valve was obtained and is shown in Fig. 5 (together with a first-order-system response for comparison). Three spools with different heights of the crescent overlap area were tested. The main structural parameters of the 2D servo valve and the spools are listed in Table 1 and 2. There is very good agreement of the first-order-system with the experimental results, except when the height of the overlap area becomes small. For small values of the height h_0 of the crescent overlap area, the leakage through the spool-to-bushing clearance has an effect on the dynamic characteristics of the valve.

Table 1: Parameters of the 2D servo valve

R	: Radius of spool land	6 mm
r_d	: Radius of hole A (B)	1.2 mm
L_V	: Length of left spool cavity	1 mm
p_s	: System pressure	21 Mpa
$x_{v \max}$: Maximum displacement	0.41 mm
β	: Pitch angle of spiral groove	45.8°

Table 2: Parameters of the spools

Spool 1		
h_0	: Overlap height of crescent area	0.03 mm
δ	: Spool-to-sleeve clearance	0.0043 mm
Spool 2		
h_0	: Overlap height of crescent area	0.06 mm
δ	: Spool-to-sleeve clearance	0.0039 mm
Spool 3		
h_0	: Overlap height of crescent area	0.11 mm
δ	: Spool-to-sleeve clearance	0.0051 mm

3 Frequency Response of Stepper Motor under Continual Control

Under the assumptions that the magnetic circuit does not saturate, and both the eddy current and the magnetic hysteresis are negligible, the voltage balance equation of the stepper motor can be established (Ruan and Burton, 1999) as follows:

$$u_m \sin Z_i(\theta_{mc} - \theta_m) = LZ_i \frac{d\theta_m}{dt} + KZ_i \cos Z_i(\theta_m - \theta) \frac{d\theta}{dt} \quad (4)$$

In Eq. (4), $u_m = \sqrt{u_A + u_B}$ and $\theta_{mc} = \frac{1}{Z_i} a \tan \frac{u_A}{u_B}$. In

this expression θ_{mc} is the control signal of the angular displacement of the rotating magnetic field θ_m . θ_m can also be regarded as the angular displacement of "rotary voltage".

The torque equation is

$$T_e = T_m \sin Z_i(\theta_m - \theta) \quad (5)$$

The torque balance equation is

$$T_e = J_g \frac{d^2\theta}{dt^2} + B_c \frac{d\theta}{dt} + T_L \quad (6)$$

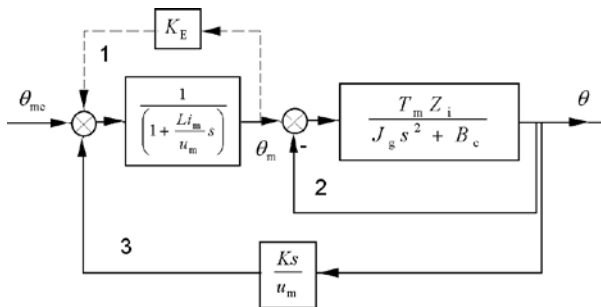


Fig. 6: Signal flow diagram of the stepper motor under continual control

Equations (4), (5), and (6) display the relation between the "rotary voltage", the rotating magnetic field,

and the angular motion of the rotator-load assembly. The signal flow diagram of the stepper motor control in the frequency domain is given in Fig. 6. The block diagram of the stepper motor consists of three loops. Loop "1" concerns the stepper motor driver with phase-current feedback control. In this case the time constant of the phase coil will be reduced by $1/(1+K_e)$ times. For a constant-voltage power supply, K_e is equal to zero; for the phase-current feedback control, K_e is large so that the effect of the phase coil impedance on the dynamic response of the stepper motor will become negligible. Loop "2" describes the mechanical dynamic response of the rotator and the attached loads. Its closed-loop form will significantly increase the magnetic stiffness of the angular displacement and thus increase the responsive ability of the stepper motor (unlike other electro-mechanical transformers, such as an electrical magnet, in which the improvement of the dynamics are achieved by an externally attached elastic element). Loop "3" is about the effect of the inductive emf, which is beneficial for increasing the damping of the stepper motor; damping is always lacking in the mechanical part of a control system.

For a stepper motor operating under a constant-current power supply, the effect of the phase coil impedance on the dynamic response of the stepper motor will become negligible. In this case, $\theta_m = \theta_{mc}$ and the transfer function of the digital valve is expressed as

$$\frac{\theta(s)}{\theta_{mc}(s)} = \frac{1}{\frac{s^2}{\omega_m^2} + 2\xi_m \frac{s}{\omega_m} + 1} \quad (7)$$

where

$$\omega_m = \sqrt{\frac{K_{m0}}{J_g}} \quad (8)$$

$$\xi_m = \frac{1}{2} \left(\frac{B_c}{\sqrt{J_g K_{m0}}} + \frac{K}{u_m Z_i \sqrt{J_g K_{m0}}} \right) \quad (9)$$

In the above equation, K_{m0} is the static magnetic stiffness of the stepper motor; $K_{m0} = T_m Z_i \cos Z_i (\theta_{m0} - \theta_0)$. $(\theta_{m0} - \theta_0)$ is dictated by the load torque T_L and is given by:

$$(\theta_{m0} - \theta_0) = \frac{1}{Z_i} a \sin\left(\frac{T_L}{T_m}\right) \quad (10)$$

It should be noted that the above linear model can effectively describe the practical dynamic characteristics of the stepper motor only under the condition that the amplitude of the input signal is much smaller than the value of the rotary tooth angle $2\pi / Z_i$. When the input signal is a sinusoidal wave ($\theta_{mc} = \theta_A \sin(\omega t)$, for instance) and the amplitude θ_A is comparable with the value of the tooth angle $2\pi / Z_i$ the static magnetic stiffness will be modified. In the response of the sinusoidal wave, $(\theta_m - \theta)$ will vary within the range

$$(\theta_m - \theta_0) - \theta_A \frac{\sqrt{4\xi_m^2 + 1}}{2\xi_m}, \quad (\theta_m - \theta_0) + \theta_A \frac{\sqrt{4\xi_m^2 + 1}}{2\xi_m}.$$

The stiffness is modified by taking the mean value within this range. Thus, the stiffness can be expressed as:

$$K_{m0} = C_k T_m Z_i \cos Z_i (\theta_{m0} - \theta_0) \quad (11)$$

C_k is the modifying coefficient;

$$C_k = 2\xi_m \sin\left(Z_i \theta_A \sqrt{4\xi_m^2 + 1} / (2\xi_m)\right) / (Z_i \theta_A \sqrt{4\xi_m^2 + 1}).$$

The relation between C_k and θ_A, ξ_m is shown in Fig. 7.

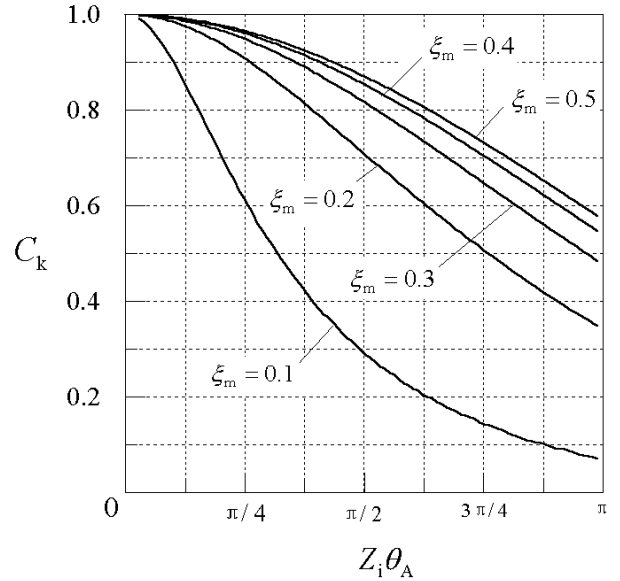


Fig. 7: C_k variation with θ_A, ξ_m

In the expression for damping ratio ξ_m , Eq. (9), the amplitude of the sinusoidal emf coefficient, K is determined through experimental measurement (Singh, G. and Kuo, B.C., 1974).

The frequency response of the stepper motor is given in Fig. 8.

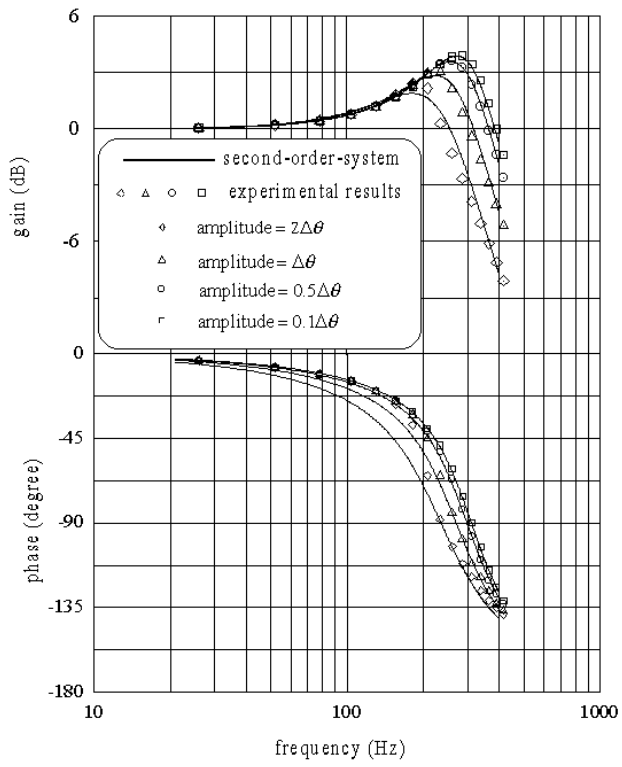


Fig. 8: Frequency response of the stepper motor

4 Continual Control of the Stepper Motor

In the design of the 2D servo valve, a small number of steps corresponding to full stroke of the spool is selected to maintain the high responding speed. The accuracy is sustained by introducing continual control of the stepper motor. There are several possible methods to achieve continual control of the stepper motor. One of them is PWM control between two adjacent stepping points. It is realized by a special control program in a micro-computer. Within each sampling cycle, the micro-computer obtains the discrete value of the continuous input signal through A/D conversion or from an upper-stage computer directly. By running the control program, the sampling signal is converted into a PWM signal. For a sinusoidal input signal, the signal conversion from the sampling signal to the PWM signal is shown in Fig. 9. The signal conversion produces an additional digital fragment. A spectral analysis displays the main energy of the fragment signal as distributed over a high frequency range (Ruan and Burton, 1999). Thus the effect of the fragment signal on the dynamic characteristics of the 2D digital servo valve is negligible. However, the existence of the fragment signal is an important approach to provide a dynamic lubrication of the spool and to reduce the friction. This is a unique feature of PWM control which distinguishes it from the other approaches of continual control of the stepper motor.

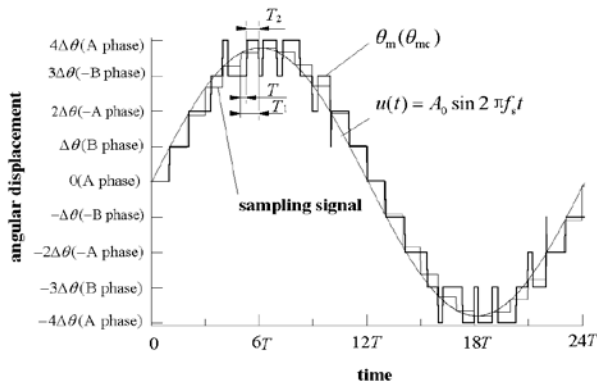


Fig. 9: Signal conversion

In order to prevent the stepper motor from losing steps, it is necessary to keep the angular difference between the magnet field and rotator within the range $(-2\pi / Z_i, 2\pi / Z_i)$. This is accomplished through limiting the rate of the rotating magnetic field. In the control program, the maximum increment is set to be θ_v between two sampling cycles T . Thus, the maximum rate limit of the rotating magnetic field is θ_v / T . The determination of the value θ_v / T is given in the Appendix.

The tracking control signal waveform will show some distortion due to the limitation of the rate of the rotating magnetic field. For convenience, a non-dimensional parameter $\lambda = 2\pi f_s A_0 T / \theta_v$ is introduced. When $\lambda \leq 1$, the rotating magnetic field θ_m

will linearly restore the input sinusoidal wave as illustrated in Fig. 10 (case A). This is because the maximum slope of the stepper motor angular displacement (with respect to time) is always greater than the instantaneous slope

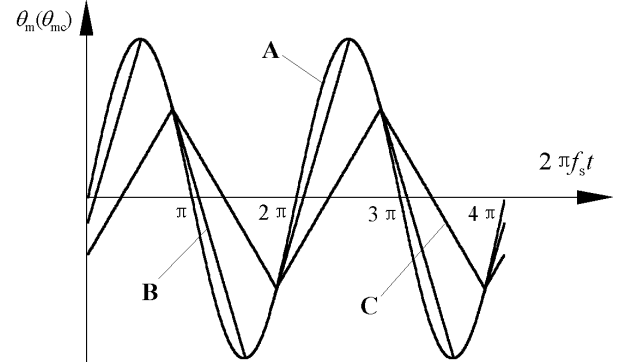


Fig. 10: Signal of the rotating magnetic field

of the input signal. Thus it can always "catch up" to the input signal at every step. When $1 \leq \lambda \leq 1.614$, the rotating magnetic field will be unable to restore the input sinusoidal wave completely and shows a distortion as case B illustrates in Fig. 10. In this case, the maximum slope of the stepper motor angular displacement (with respect to time) is less than the slope of the input signal and hence cannot catch up to the desired input signal. Thus the slope will stay constant until it finally catches up to the input signal. When $\lambda > 1.614$ the wave of the rotating magnetic field will diverge completely from the sinusoidal wave and become a triangular signal with a phase delay with respect to the input sinusoidal wave (see case C of Fig. 10). The frequency response for the nonlinear digital control is obtained by using the describing function method (Ruan and Burton, 1999b). It is shown in Fig. 11.

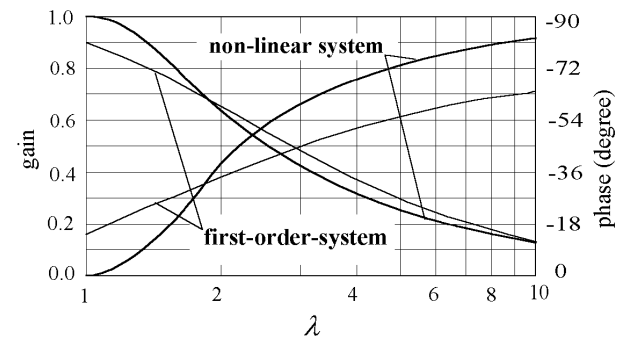


Fig. 11: Frequency response for continual control

The digital control of the stepper motor may be approximated using a first-order-system as follows:

$$\frac{\theta_m(s)}{U(s)} = \frac{1}{\tau s + 1} \tag{12}$$

The time constant, τ , is evaluated at the point $\lambda = 1.614$ corresponding to the gain of 0.701.

$$\tau = \frac{3.88 T A_s}{\theta_v} \tag{13}$$

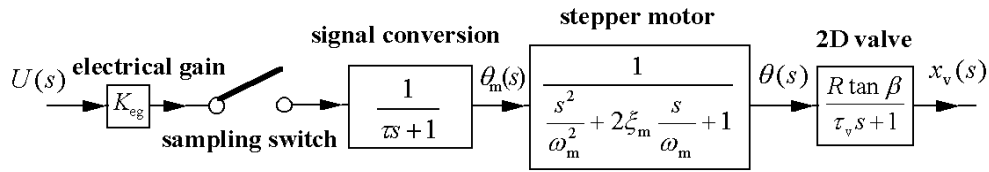


Fig. 12: Flow diagram of the 2D digital servo valve

5 Frequency Response of Digital Servo Valve

The frequency domain model of the 2D digital servo valve is given in Fig. 12. It is composed of three parts: The first is the signal conversion which is due to the limitation to the rotary speed of the stepper motor and is described as a first-order system. The second is the stepper motor which is described as a second-order system under the constant-current power supply (which is concurrently the most popular method for the power supply of stepper motor). The third is the 2D servo valve. Because the left spool cavity is limited to a small size and thus the compressibility of oil can be neglected, the control of the 2D servo valve is simplified as a first-order system. Finally, the transfer function for the continual part is:

$$G(s) = \frac{X_v(s)}{\theta_{mc}(s)} = \frac{R \tan \beta}{(\tau_s s + 1) (\tau_v s + 1) \left(\frac{s^2}{\omega_m^2} + 2 \zeta_m \frac{s}{\omega_m} + 1 \right)} \quad (14)$$

The frequency response of the 2D digital servo valve is shown in Fig. 13. For discrete control, the theoretical results for gain and phase are obtained from $|G(j\omega) - G(j(\omega + 2\pi/T))|$ and $\angle(G(j\omega) - G(j(\omega + 2\pi/T)))$ respectively. The main physical parameters of the 2D digital valve, stepper motor and the controller are given in Tables 3, 4 and 5.

Table 3: Physical parameters of the 2D digital valve

h_0	: Overlap height of crescent area	0.03 mm
p_s	: System pressure	21 Mpa
Q_L	: Max. flow rate $p_A - p_B = 3.5$ Mpa	40 l/min
N_0	: Max. step number	± 8 Steps
h_0	: Height of crescent overlap area	0.11 mm
$x_{v \max}$: Maximum displacement	0.41 mm
r_d	: Radius of high and low pressure hole	1.2 mm
β	: Pitch angle of spiral groove	45.8 °

Table 4: Physical parameters of the stepper motor

V_0	: Voltage of power supply	24 V
I_0	: Max. Current consumption	0.45 A
i_0	: Max. Phase current	2 A
T_m	: Max. torque	0.18 Nm
J_g	: Rotary inertia of rotary-spool assembly	1.5 $\cdot 10^{-5}$ kgm ²
Z_1	: Number of teeth of rotator	50
$\Delta\theta$: Step length	0.9 °

Table 5: Physical parameters of the controller

T	: Sampling cycle	0.5 ms
θ_v	: Max. increment of angle	0.9 °

The bandwidth of the 2D digital servo valve will decrease as the amplitude of the input signal increases. The bandwidth for an amplitude of 25 % of the spool's full stroke is about 310 Hz corresponding to a -3 dB gain. The value will drop to 81 Hz when the amplitude is at full spool stroke. The reason for the decrease of the bandwidth is due to the limitation of the rate of the rotating magnetic field. The time constant for signal conversion increases with the amplitude of the input signal, as demonstrated in Eq. (13). The theoretical results agree well with the experimental ones, except at lower frequencies where the theoretical results have somewhat lower values than the experimental ones. This difference is caused by the approximation of the digital control with the first-order-system. When the non-dimensional frequency parameter λ is smaller than 1, the sinusoid is restored without any attenuation in amplitude. But for a first-order-system, the amplitude is somewhat decreased.

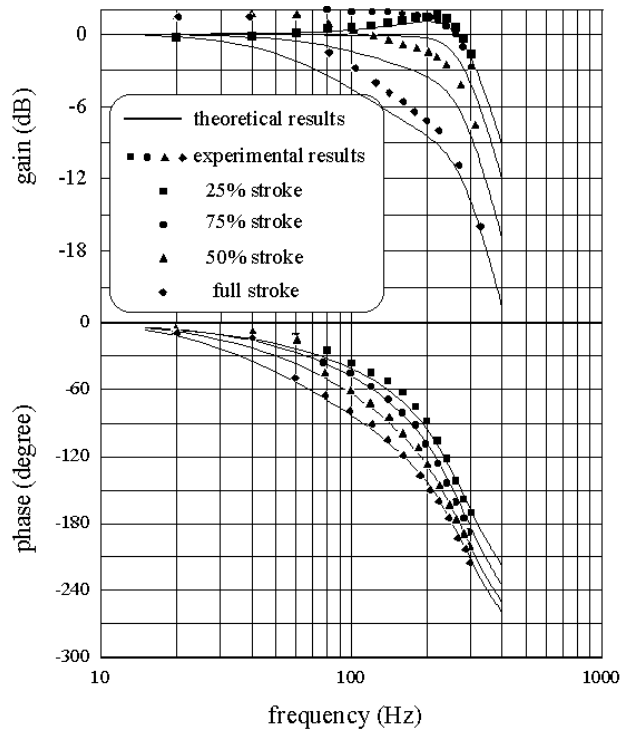


Fig. 13: Frequency response of 2D digital servo valve

6 Conclusion

The control model of the 2D digital servo valve consists mainly of three parts: the 2D valve, the stepper motor, and the control signal conversion part. The 2D valve is essentially a mechanical servo device. Because of the large value of the hydraulic natural frequency, the second-order-system of the open loop velocity control has little influence on the dynamic characteristics of the valve and the 2D valve is approximated as a first-order-system. The dynamic characteristics of the stepper motor are to a large extent dictated by the type of power supply used. For a constant-current supply, the stepper motor is identified as a second-order-system. In order to prevent the stepper motor from losing steps, the rate of the rotating magnetic field is limited. This will cause performance deterioration under inputs of large amplitude and high frequency. The non-linearity associated with this is approximately described as a first-order-system. Because of the limitation to the rate of the rotating magnetic field, the frequency responding ability will drop as the amplitude of the input signal increases. Experiments show that the bandwidth of the 2D digital servo valve is about 310 Hz for an amplitude of 25 % of the spool's full stroke. This value decreases to 81 Hz when the amplitude is that of full stroke.

Appendix: Maximum Slope of the Magnetic Control Signal

Corresponding to the input sinusoidal signal, $u = A_0 \sin(\omega t)$, the difference between the angular displacement of the rotating magnetic field and the rotator is

$$\phi = A_m (\sin(\omega t - \alpha) - \gamma \sin g(\omega t - \alpha - \beta)) \quad (15)$$

In above equation is:

A_m : amplitude of the rotating magnetic field

$$A_m = \frac{A_0}{\sqrt{\tau^2 \omega^2 + 1}} \quad (16)$$

α : phase difference between the magnetic field control signal and the rotating magnetic field

β : phase difference between the rotating magnetic field and the rotator

$$\beta = a \tan \left(\frac{4\xi_m \frac{\omega}{\omega_m}}{1 - \frac{\omega^2}{\omega_m^2}} \right) \quad (17)$$

γ : Amplitude ratio of angular displacement between rotator and rotary magnetic field

$$\gamma = \frac{1}{\sqrt{(1 - \frac{\omega^2}{\omega_m^2})^2 + 4\xi_m^2 \frac{\omega^2}{\omega_m^2}}} \quad (18)$$

In order to prevent the stepper motor from losing steps, the angular difference between the rotating

magnetic field and the rotator must be keep within range $(-\pi/Z_i, \pi/Z_i)$ at the point when the velocity of the rotator is equal to zero.

$$\text{When } \frac{d\phi}{dt} = 0, \quad |\phi| < \pi/Z_i \quad (19)$$

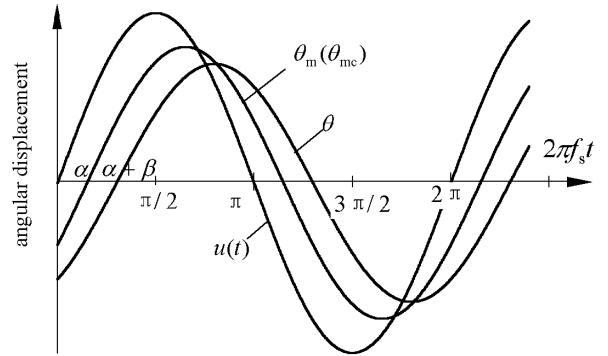


Fig. 14: Response to the input sinusoidal wave

With reference to Fig. 14 (for the sinusoidal wave), at the points $\omega t = \alpha + \beta + \pi/2 + i\pi$ ($i = 0, 1, 2, 3, \dots$), the velocity of the rotator is equal to zero. Thus, Eq. (15) is rewritten as

$$A_m (\cos \beta - \gamma) < \pi/Z_i \quad (20)$$

Substituting Eq. (16), (17) and (18) in Eq. (20) gives

$$\frac{A_0}{\sqrt{\tau^2 \omega^2 + 1}} \frac{\frac{\omega^2}{\omega_m^2}}{\sqrt{(1 - \frac{\omega^2}{\omega_m^2})^2 + 4\xi_m^2 \frac{\omega^2}{\omega_m^2}}} < \frac{\pi}{Z_i} \quad (21)$$

When the frequency of the sinusoidal wave, ω , is equal to natural frequency of the stepper motor, ω_m , the left side of the inequality reaches its maximum. Thus, the inequality is rewritten as

$$\frac{A_0}{\sqrt{\tau^2 \omega_m^2 + 1}} \frac{1}{2\xi_m} < \frac{\pi}{Z_i} \quad (22)$$

Consider the case when $\tau\omega_m > 1$ and substitute $\tau = \frac{3.88 T A_0}{\theta_v}$ into the left side of Eq. (22). The limi-

tation of the slope of the magnetic control signal, $\frac{\theta_v}{T}$, is then obtained as

$$\frac{\theta_v}{T} < \frac{7.76 \pi \xi_m \omega_m}{Z_i} \quad (23)$$

Nomenclature

A_0	Amplitude of input sinusoidal wave	[V]
A_s	End area	[m ²]
B_c	Coefficient of viscous frictional torque	[Ns/m]
C_d	Coefficient of the flow rate	[]
C_k	Modifying coefficient of stiffness	[]

F	Coulomb frictional force	[N]
h_0	Initial overlap size of crescent area	[m]
I_0	Maximum Current consumption	[A]
i_0	Maximum Phase current	[A]
i_A, i_B	Coil current of phase A and B	[A]
f_s	Frequency of input signal	[Hz]
J_g	Rotary inertia of rotator-spool assembly	[kgm ²]
K	Amplitude of sinusoidal emf coefficient	[V]
K_e	Volumetric modular	[Pa]
K_E	Coefficient of current feedback	[V/A]
K_{eg}	Gain of electrical part	[]
K_p	Flow-pressure coefficient	[m ³ /Pas]
K_v	Flow rate gain	[m ² /s]
K_λ	Modifying coefficient of non-linear crescent overlap area	[]
L	Impedance of phase coil	[H]
L_V	Depth of spool left chamber	[m]
p_A, p_B	Pressure of Port A and B	[Pa]
p_s	Pressure of system	[Pa]
r_d	Radius of holes A or B	[m]
R	Radius of spool land	[m]
t	Time	[s]
T	Sampling cycle	[s]
T_e	Output torque of stepper motor	[Nm]
T_L	Load torque	[Nm]
T_m	Maximum output torque of stepper motor	[Nm]
u_A, u_B	Voltage of phases A and B	[V]
V_0	Voltage of power supply	[V]
V_c	Volume of left spool cavity	[m ³]
x_v	Displacement of spool	[m]
Z_i	Number of teeth of rotator	[]
β	Pitch angle of spiral groove	[°]
$\Delta\theta$	Step length	[°]
λ	Non-dimensional frequency parameter	[]
θ	Rotary angle of spool	[°]
θ_A	Amplitude of sinusoidal motion of stepper motor	[°]
θ_m	Angular displacement of rotating magnetic field	[°]
θ_{mc}	Control signal of rotating magnetic field	[°]
θ_v	maximum increment of control signal	[°]
ρ	Density of oil	[kg/m ³]
τ	Time constant of digital control	[s]
τ_v	Time constant of 2D valve	[s]
ω_h	Hydraulic natural frequency	[rad/s]
ω_m	Natural frequency of stepper motor	[rad/s]
ξ_h	Hydraulic damping ratio of	[]
ξ_m	Damping of stepper motor	[]

References

- Hesse and Moller** 1972. Pulsemodulierte Steuerung von Magnetventilen. *O+P (Ölhydraulik und Pneumatik)*, Vol. 16.
- Hou, Y., Burton, R., Schoenau, G. and Muto, T.** 1995. Feasibility Study on the Development of an Ultra High Speed On-off Valve. *Proceedings of the 4th Scandinavian International Conference*, pp. 673-685.
- Lai, J. Y., Menq, C. H., and Singh, R.** 1989. Pressure Control of a Pneumatic Chamber. *Journal of Fluid Power Control*, Vol 13, pp. 64-76.
- Merritt, H. E.** 1967. *Hydraulic Control Systems*. John Wiley & Sons, New York.
- Palanisamy, K. R.** 1981. System Identification via Block-pulse Functions. *Journal of System Science*, Vol. 12, pp. 643-647.
- Ramachandran, S., Ukrainetz, P. R. and Nikiforuk P. N.** 1985. Digital Flow Control Valve-an Evaluation. *Proceedings of the First International Conference on Fluid Power Transmission and Control*, Hangzhou, China, pp. 508-512.
- Ruan, J. and Burton, R. T.** 1999a. Direct Digital Control of a 2D Directional Valve. *Proceedings of the Sixth Scandinavian Conference on Fluid Power*, Tampere, Finland, pp. 1335-1348.
- Ruan, J. and Burton, R.** 1999b. A New Approach of Direct Digital Control for Spool Valves. *The 1999 ASME International Mechanical Engineering Congress*, Fluid Power Systems Technology, FPST-Vol.6, pp. 135-144.
- Ruan, J., Burton, R. and Ukrainetz, P.** 2000. Investigation to the characteristics of 2D flow valve. *The 2000 ASME International Mechanical Engineering Congress*, Fluid Power Systems Technology, Orlando, USA.
- Sawamura, T. and Anafusa, H.** 1962. Stability Problems of a Servomechanism Operated by PWM Mode (Part II, The Case When a Feedback Circuit Consists of a Proportional Element). *Trans. JSME*, Vol. 28, pp. 542-550.
- Singh, G. and Kuo, B. C.** 1974. *Modeling and Dynamic Simulation of Multiple-stack Variable-Reluctance Step Motors*. Computers and Electrical Engineering, Vol. 1, pp. 481-500.
- Tsai, S. C. and Ukrainetz, P. R.** 1970. Response Characteristics of a Pulse-width-modulated Electro Hydraulic Servo. *Trans. ASME, J. Basic Eng.*, pp. 204-214.
- Xu, Y. M. and Ruan, J.** 1989. Study of a New Type of Electro-pneumatic Digital Pressure Valve. *Proceedings of the First Japanese Conference on Fluid Power Control and Measurement*, Tokyo, Japan, pp. 107-112.

Jin, Y. 1997. Simulation Study of an Electro-hydraulic Digital Compound Valve. *Proceedings of the 4th International Conference on Fluid Power Transmission and Control*, Hangzhou, P. R. China, pp. 165-168.



Richard Burton

Born Sept. 6, 1947.

Richard Burton is a Professor of Mechanical Engineering at the University of Saskatchewan, Saskatoon, Canada and is now Assistant Dean of Undergraduate Studies at this same institution. He received his B.E degree in Engineering Physics and M.Sc. and Ph.D. in Hydraulic Controls from the Univ. of Saskatchewan. He has been and continues to be active in research in the Fluid Power area. He is a member of the ASME (FPST), SAE and NCFP Advisory Boards. He is also convenor for FPN (Canada).



Paul Ukrainetz

BE. 1957 U of S, M.Sc. 1960 Univ. of British Columbia, Ph.D. 1962 Purdue University Bristol Aeroplane Co. 1957
U of S Assistant Professor 1962
U of S Associate Professor 1966
U of S Full Professor 1971
Head Department of Mechanical Engineering, U of S. 1974 – 1982, Professor Emeritus, 1999 - date. Active in Fluid Power Systems since 1962.



Jian Ruan

Born on April 4th 1963 in Fuan City of Fujiang Province, P.R. China. Receiving Ph. D. from Harbin Institute of Technology in Sept. 1989. Study of electro-hydraulic (pneumatic) direct digital control components and systems. Post-doctoral fellow of FPTC, Zhejiang University. Professor of Mechanical Engineering at Zhejiang University of Technology